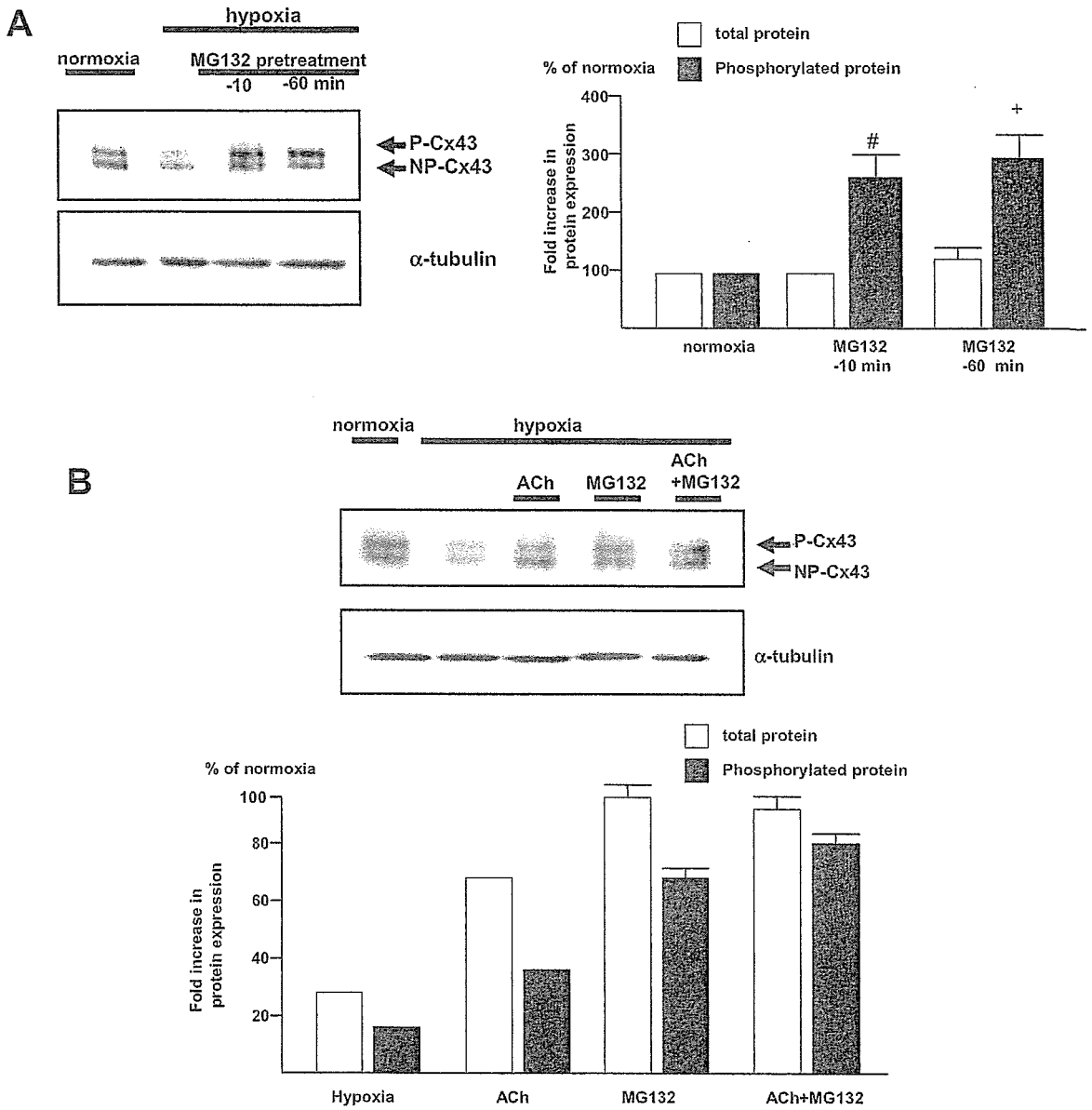

Fig. 4. MG132, a proteasome inhibitor, increases the Cx43 protein level during hypoxia, and cotreatment with ACh does not change this effect. A: Pretreatment with MG132 inhibits the reduction in Cx43 phosphorylation induced by hypoxia ($^{\#}P<0.05$ *vs* normoxia; $^{+}P<0.05$ *vs* normoxia, n = 5). Normoxia: no MG132 or hypoxia. The cells were pretreated with 10 μmol/L MG132 before and at 10 and 60 min of hypoxia. B: The effect of MG132 on inhibiting the reduction in Cx43 phosphorylation is not accentuated by cotreatment with 1 mM ACh since the level of Cx43 phosphorylation with ACh + MG132 is comparable to that with MG132 alone (not significant *vs* MG132, n = 5). Representative data from 5 independently performed experiments are shown (n = 5).

under hypoxia, to the same level observed under normoxia. On the basis of the finding that the survival of Cx43 knockout mice was extremely poor due to ventricular arrhythmia (9, 10), it is suggested that ACh regulates Cx43, which may inhibit arrhythmia.

Our immunohistochemical study supported the result that ACh greatly suppressed the reduction in the Cx43 level under hypoxia. L-NAME inhibited the effect of ACh on Cx43, whereas SNAP mimicked the ACh effect, suggesting that NO is involved in the signaling pathway. ACh is able to induce NO production (17) and has a cardioprotective effect both in vivo and in vitro (18, 19). In fact, H9c2 cells were reported to generate NO from mitochondria in response to ACh (20). Taken together,

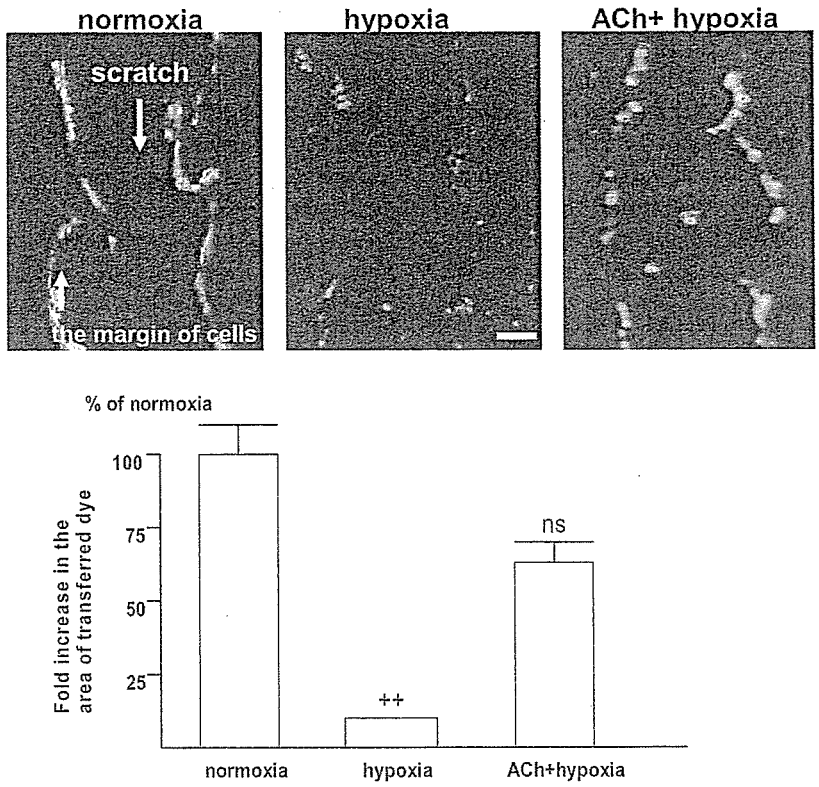

Fig. 5. Fluorescence photomicrographs of scrape/scratch experiments using Lucifer Yellow. Intercellular communication is blocked in H9c2 cells treated with 60 min of hypoxia (hypoxia) ($^{++}P<0.01$ *vs* hypoxia, n = 5). ACh (1 mM) reverses the blockage of intercellular communication induced by hypoxia (ACh + hypoxia) to a comparable level to the control (ns, not significant *vs* normoxia; n = 5) Bar: 150 μm.

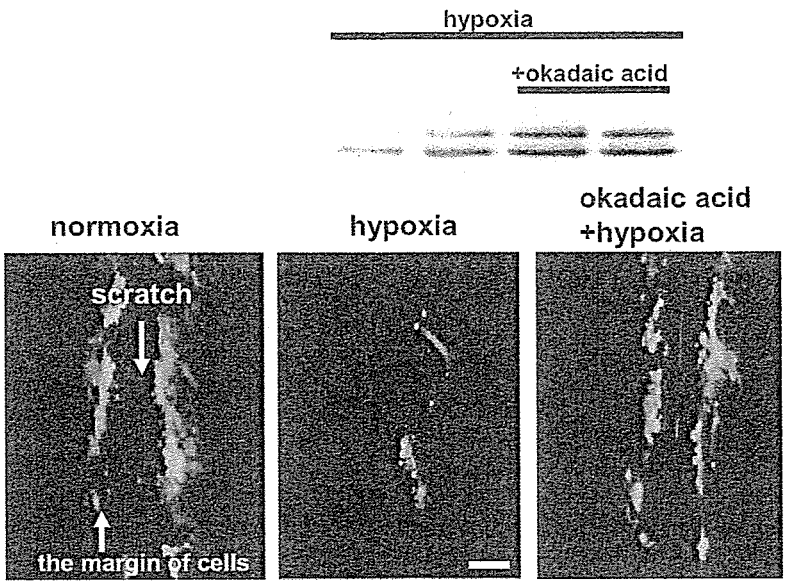

Fig. 6. Phosphatase inhibition recovers cell-cell communication during hypoxia. Pretreatment with okadaic acid (1 μm) for 10 min before hypoxia inhibits the reduction in the Cx43 protein level during hypoxia. Furthermore, it reverses the dye transfer blockage under hypoxia, similar to ACh. Representative data from 3 independently performed experiments are shown (n = 3). Bar: 150 μm.

it is suggested that ACh regulates the Cx43 protein level in cardiomyocytes partly through NO.

To explore whether the Cx43 level during hypoxia was regulated by proteasome degradation, we treated cells with the proteasome inhibitor MG132. Recently, several types of low-molecular-weight proteasome inhibitors have been developed that can readily enter cells and selectively inhibit the protein-degradation pathway. Although their toxicities may sometimes be troublesome experimentally, cell viability and growth are not generally affected by short treatments with these molecules (21 – 23). Surprisingly, MG132 increased the Cx43 protein level, which was reduced under hypoxia, to a comparable level to that after ACh treatment. However, the effect of MG132 on the recovery of Cx43 was not affected by cotreatment with ACh. These results suggest that the proteasome pathway plays a role in Cx43 degradation and that ACh modulates the degradation of Cx43 during hypoxia.

The results of the present study have demonstrated that the increased Cx43 protein level contributes to the functional improvement of gap junctions under hypoxia using the scrape/scratch method. The ACh-induced increase in the Cx43 protein level was functionally involved in the cell-cell communication since ACh recovered Lucifer Yellow transport from the margin of the scratched regions, even under in hypoxia.

As well as the total protein level, the Cx43 phosphorylation level was shown to be involved in its function. Specifically, okadaic acid, a phosphatase inhibitor, recovered the Cx43 protein level and the extent of dye transfer under hypoxia, suggesting that dephosphorylation was partially involved in the hypoxia-induced degradation, eventually leading to a decrease in the total Cx43 protein level. To date, several phosphorylation sites of Cx43 have been reported to have positive or negative effects on gap junctions, suggesting that their function depends on these phosphorylation sites (24). Although we did not investigate the specific phosphorylation site regulated by ACh in the present study, our results suggest that ACh modulates the function of gap junctions through both the protein and phosphorylation levels of Cx43.

Although the scrape/scratch method has some limitations for evaluating cell-cell communication, the result obtained were compatible with those in our previous dye injection study under chemical hypoxia, that is, ACh-treated cardiomyocytes efficiently transferred the dye to surrounding cells, even under hypoxia (4). Therefore, these results suggest that inhibition of the decrease in the Cx43 protein level by ACh under hypoxia is responsible for the enhanced cell-cell communication.

H9c2 cells have been shown to retain several characteristics of the electrical and hormonal signaling pathways found in adult cardiomyocytes and are therefore a useful model for cardiomyocytes from the aspect of signal transduction. The cells show similar morphological characteristics to immature embryonic cardiomyocytes (20).

In conclusion, the results of the present study suggest that ACh activates cell-cell communication by sustaining the Cx43 protein level during hypoxia through modification of the Cx43 degradation pathway.

Acknowledgment

This study was supported by a Health and Labor Sciences Research Grant (H15-PHYSI-001) for Advanced Medical Technology from Ministry of Health, Labor, and Welfare of Japan.

References

1 Janse MJ. Electrophysiological changes in heart failure and their relationship to arrhythmogenesis. Cardiovasc Res. 2004;61:208–217.
2 Prado MAM, Reis RAM, Prado VF, de Mello MC, Gomez MV, de Mello PG. Regulation of acetylcholine synthesis and storage. Neurochem Int. 2002;41:291–299.
3 Li M, Zheng C, Sato T, Kawada T, Sugimachi M, Sunagawa K. Vagal nerve stimulation markedly improves long-term survival after chronic heart failure in rats. Circulation. 2004;109:120–124.
4 Ando M, Katare GR, Kakinuma Y, Zhang D, Yamasaki F, Muramoto K, et al. Efferent vagal nerve stimulation protects heart against ischemia-induced arrhythmias by preserving connexin43 protein. Circulation. 2005;12:164–170.
5 Musil LS, Goodenough DA. Biochemical analysis of connexin43 intracellular transport, phosphorylation, and assembly into gap junctional plaques. J Cell Biol. 1991;115:1357–1374.
6 Lamp PD, Lau AF. Regulation of gap junctions by phosphorylation of connexins. Arch Biochem Biophys. 2000;384:205–215.
7 Moon C-H, Jung Y-S, Kim MH, Park RM, Lee SH, Baik EJ. Protein kinase C inhibitors attenuate protective effect of high glucose against hypoxic injury in H9c2 cardiac cells. Jpn J Physiol. 2000;50:645–649.
8 Jain SK, Schuessler RB, Saffitz JE. Mechanisms of delayed electrical uncoupling induced by ischemic preconditioning. Circ Res. 2003;92:1138–1144.
9 van Rijen HV, Eckardt D, Degen J, Theis M, Ott T, Willecke K, et al. Slow conduction and enhanced anisotropy increase the propensity for ventricular tachyarrhythmias in adult mice with induced deletion of connexin43. Circulation. 2004;109:1048–1055.
10 Gutstein DE, Morley GE, Vaidya D, Liu F, Chen FL, Stuhlmann H, et al. Conduction slowing and sudden arrhythmic death in mice with cardiac-restricted inactivation of connexin43. Circ Res. 2001;88:333–339.

11 Hescheler J, Meyer R, Plant S, Krautwurst D, Rosenthal W, Rosenthal W, et al. Morphological, biochemical, and electrophysiological characterization of a clonal cell (H9c2) line from rat heart. Circ Res. 1991;69:1476–1486.
12 Le A-CN, Musil LS. Normal differentiation of cultured lens cells after inhibition of gap junction-mediated intercellular communication. Dev Biol. 1998;204:80–96.
13 Musil LS, Le A-CN, Vanslyke JK, Roberts LM. Regulation of connexin degradation as a mechanism to increase gap junction assembly and function. J Biol Chem. 2000;275:25207–25215.
14 McNeil PL, Murphy RF, Lanni F, Taylor DL. A method for incorporating macromolecules into adherent cells. J Cell Biol. 1984;98:1556–1564.
15 El-Fouly MH, Trosko JE, Chang C-C. Scrape-loading and dye transfer. A rapid and simple technique to study gap junctional intercellular communication. Exp Cell Res. 1987;168:422–430.
16 Stewart WW. Functional connections between cells as revealed by dye-coupling with a highly fluorescent naphthalimide tracer. Cell. 1978;14:741–759.
17 Liu H, Mcpherson BC, Zhu X, Da Costa MA, Jeevanandam V, Yao Z. Role of nitric oxide and protein kinase C in ACh-induced cardioprotection. Am J Physiol Heart Circ Physiol. 2001;281: H191–H197.
18 Rakhit R, Edwards RJ, Mockridge JW, Baydoun AR, Wyatt AW, Mann GE, et al. Nitric oxide, nitrates and ischaemic preconditioning. Am J Physiol Heart Circ Physiol. 2000;278: H1211–H1217.
19 Monastyrskaya E, Folarin N, Malyshev I, Green C, Andreeva L. Application of the nitric oxide donor SNAP to cardiomyocytes in culture provides protection against oxidative stress. Nitric Oxide. 2002;7:127–131.
20 Zanella B, Calonghi N, Pagnotta E, Masotti L, Guarnieri C. Mitochondrial nitric oxide localization in H9c2 cells revealed by confocal microscopy. Biochem Biophys Res Commun. 2002;290:1010–1014.
21 Lee DH, Goldberg AL. Proteasome inhibitors: valuable new tools for cell biologists. Trends Cell Biol. 1998;8:397–403.
22 Laing JG, Beyer EC. The gap junction protein connexin43 is degraded via the ubiquitin proteasome pathway. J Biol Chem. 1995;270:26399–26403.
23 Lampe PD, Tenbroek EM, Brut JM, Kurata WE, Johnson RG, Lau AF. Phosphorylation of connexin43 on serine368 by protein kinase C regulates gap junctional communication. J Cell Biol. 2000;149:1503–1512.
24 Lampe PD, Lau AF. The effects of connexin phosphorylation on gap junctional communication. Int J Biochem Cell Biol. 2004;36:1171–1186.

バイオニック治療戦略

高知大学循環制御学　佐藤隆幸（さとうたかゆき）
九州大学大学院医学研究院循環器内科学　砂川賢二（すながわけんじ）

はじめに

循環器疾患では，心不全や圧反射失調のように制御機構の機能破綻が病態の悪化や予後を規定する因子になることがある．そこで，積極的に循環制御機構の機能再建や最適化を図るための新しい治療戦略として，神経インターフェイス技法を用いたバイオニック療法が提唱されている[1]．

本稿では迷走神経の電気刺激による心不全治療[2]に関する実験的研究，および脊髄交感神経刺激による術中自動血圧制御に関する臨床研究[3]について紹介する．

迷走神経刺激による慢性心不全治療

最新の病態に関する研究により，慢性心不全の重要な予後規定因子として，循環調節機構の破綻があげられている．当初は，心機能低下の代償機転として適応的にはたらいていた交感神経系の活性化と副交感神経系の活動低下やレニン・アンジオテンシン系の活性化が，次第に心臓リモデリングを進展・悪化させ，一種の悪循環を形成し，最終的には調節破綻に陥ると考えられるようになってきた．さらに，大規模臨床試験により，呼吸性心拍変動の低下や心拍数増加が予後不良因子として認識されるようになった．これらはいずれも心臓迷走神経活動の低下を反映したものである[4~8]．そこで，「迷走神経を電気刺激する神経インターフェイス療法」が生命予後を改善するか否かを心不全モデル動物を用いて実験的に検証した．

左冠動脈起始部の結紮により，左室の40～50％が梗塞に陥った慢性心不全ラットの右迷走神経に刺激電極を固定し，植え込み型電気刺激装置と接続した．刺激強度は心拍数が10～20％低下する程度にした．迷走神経刺激療法は6週間でうち切り，血行動態・心臓リモデリングに与える影響と140日間の長期生存率を観察した．

1.　心機能およびリモデリングに与える影響

図1は治療終了時の血行動態の比較を示している．血圧は，梗塞後心不全群は健常群に比べ有意に低かった．梗塞後心不全群は，健常群に比べ左室拡張末期圧の有意な上昇と左室圧一次微分最大値の有意な低下を示したが，迷走神経刺激療法により，左室拡張末期圧の有意な減少と左室圧一次微分最大値の有意な上昇が認められた．両心室重量が，梗塞後心不全群では有意な増加を示したが，迷走神経刺激療法により有意に減少した．以上の結果は，6週間の迷走神経刺激療法によってポンプ機能が改善し心室リモデリングが予防されたことを示唆する．

[Key words]　循環調節，迷走神経，交感神経，神経インターフェイス

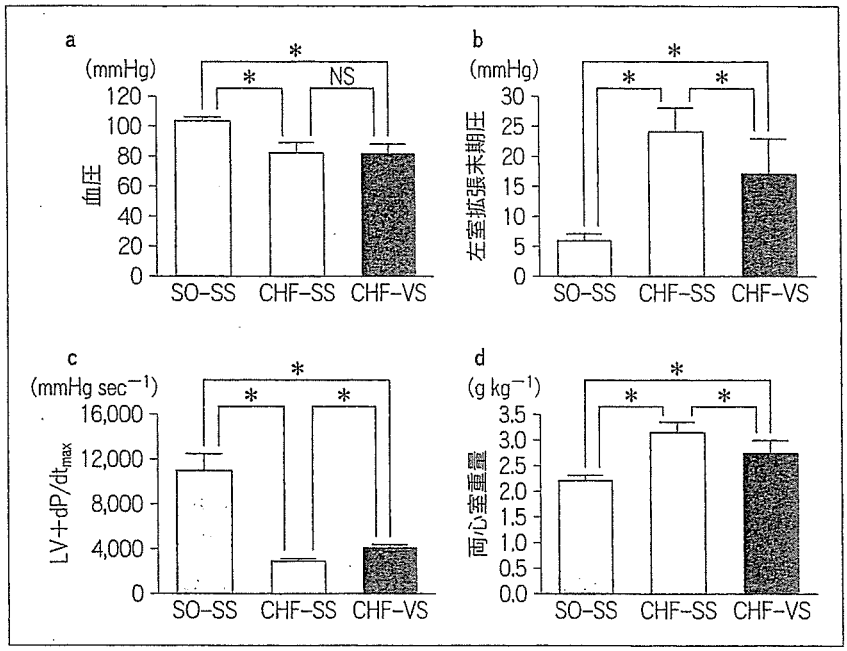

図1　迷走神経刺激の血行動態および両心室重量に与える影響

健常群（SO-SS, n=9），梗塞後心不全における非刺激群（CHF-SS, n=13）および梗塞後心不全における刺激群（CHF-VS, n=11）．数値は平均±標準偏差で示している．*p<0.05.

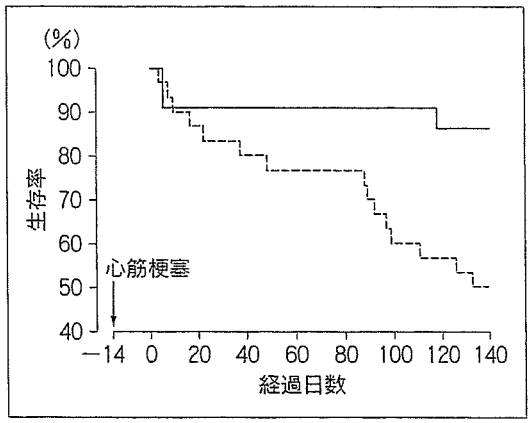

図2　迷走神経刺激の慢性心不全ラットの生存率に与える影響

実線は刺激群（n=22），破線は非刺激群（n=30）を示す．迷走神経刺激により生存率は有意に改善した（p=0.008）．

期間における生存率曲線を図2に示す．刺激群22例のうち死亡は3例，非刺激群30例のうち死亡は15例であった（p=0.008）．このように，迷走神経刺激療法は相対的死亡リスクを73％も減少させた．この効果は，アンジオテンシン変換酵素阻害薬によるものよりもさらに良好な成績であった[9]．

迷走神経刺激療法は，両心室重量，血漿ノルエピネフリンおよび脳性ナトリウム利尿ペプチドを有意に減少させた．なお，これらの指標はいずれも臨床試験で明らかにされている予後規定因子で，高値ほど予後不良とされているものである．

以上より，迷走神経刺激療法が心機能の改善とリモデリングを予防し，さらに，長期予後を著明に改善することが明らかになった[2]．

2.　長期生存率および液性因子に与える影響

迷走神経刺激療法の生存率に与える影響をKaplan-Meier法により解析した．140日の観察

3.　迷走神経刺激による抗リモデリング機序

迷走神経刺激により，不全心で生ずるリモデリングが予防される機序として，徐脈によりエネル

ギー効率の改善[10]，冠循環における血管内皮機能の改善[11]などが考えられるが，不明なところも多い．最近，筆者らは，迷走神経の末端から放出されるアセチルコリンが心筋細胞に与える影響について調べたところ，アセチルコリンがムスカリン受容体を介して，低酸素誘導因子 HIF-1α の発現を促進し，不全心でみられるアポトーシスを防止する可能性があることを報告した[12]．また，末期心不全における致死性不整脈との関連が示唆されているギャップ結合の機能低下を迷走神経刺激が防止する可能性があることを示した[13]．おもしろいことに，これらの迷走神経あるいはアセチルコリンの心筋細胞に与える効果は，徐脈効果とは独立した機序である可能性がある．

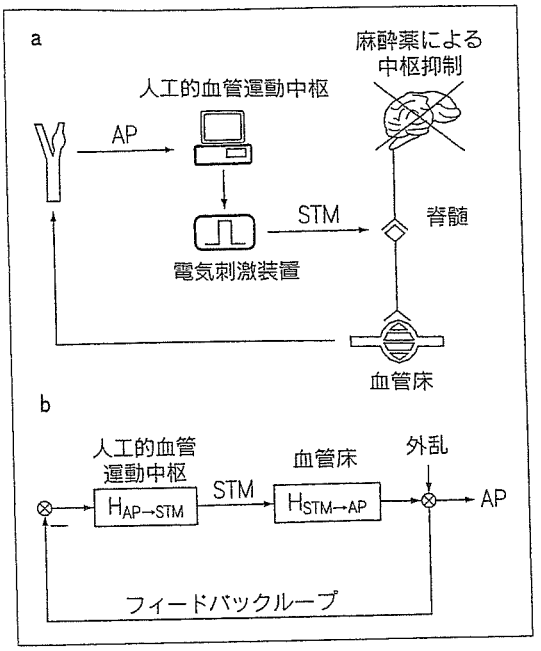

図3　バイオニック圧反射装置
バイオニック圧反射装置の概要（a）とブロック線図（b）．APとSTMはそれぞれ血圧と電気刺激を示す．

脊髄交感神経刺激による術中血圧の自動制御

動脈圧受容器反射は短期血圧調節にきわめて重要な役割を果たしているが[14,15]，多くの麻酔薬が

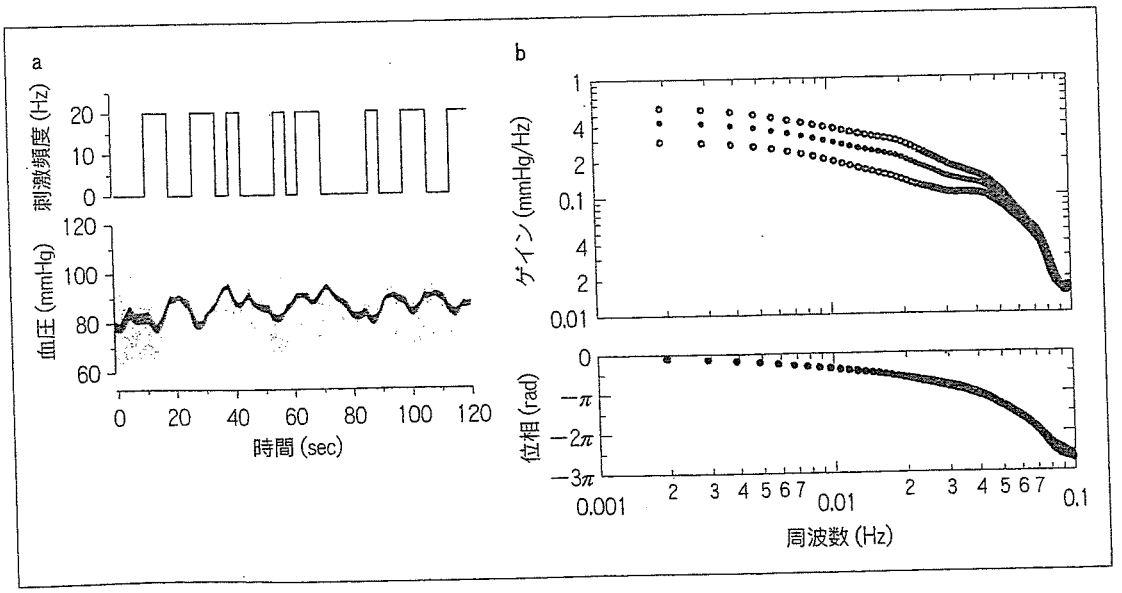

図4　脊髄交感神経の不規則刺激の例と伝達関数
a：不規則な電気刺激に対する血圧の応答は緩徐である．
b：電気刺激に対する血圧応答に関する伝達関数（$n=12$）．伝達関数により刺激に対する動脈圧応答が定量的に推定可能になる．数値は平均(●)±標準偏差(○)で示している．

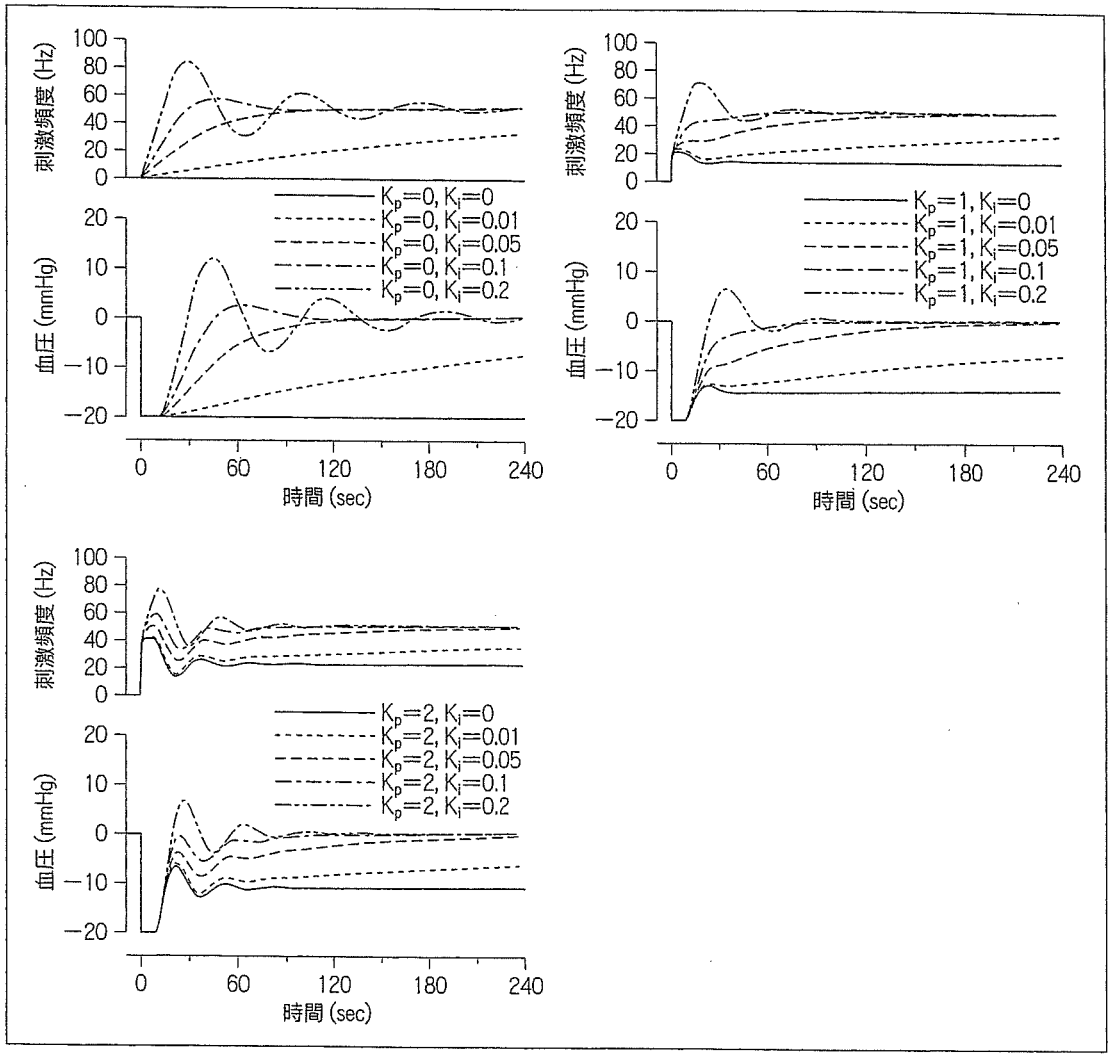

図5　数値シミュレーションによる人工的血管運動中枢の補償係数パラメータの決定
K_p と K_i はそれぞれ，比例補償係数と積分補償係数を示す．

この機能を抑制するため[16,17]，少量の出血などでも予期せぬ血圧低下をきたすことがある[18,19]．そこで，図3のように，圧センサー→コンピュータ→電気刺激装置→硬膜外カテーテル電極を用いたバイオニック圧反射装置（bionic baroreflex system: BBS）を用いて，血圧の自動制御を試みた．

1.　動作原理の開発戦略

サーボコントロールの原理を応用してBBSを試作した．サーボコントローラの動作原理としては，いわゆる，比例・積分補償型のネガティブフィードバックを採用した[20]．被制御変数である瞬時血圧 $AP(f)$ の標的血圧 $AP_t(f)$ からの偏差，すなわち，制御誤差 $E(f)$ は，$E(f)=AP_t(f)-AP(f)$ と表される．$E(f)$ から脊髄交感神経刺激 $STM(f)$ までの伝達関数 $H_1(f)$ は，比例補償係数 K_p と積分補償係数 K_i および Laplace 演算子 $s=2\pi fj$ を用いると次のように表される．

$$H_1(f)=K_p\frac{K_i}{s}$$

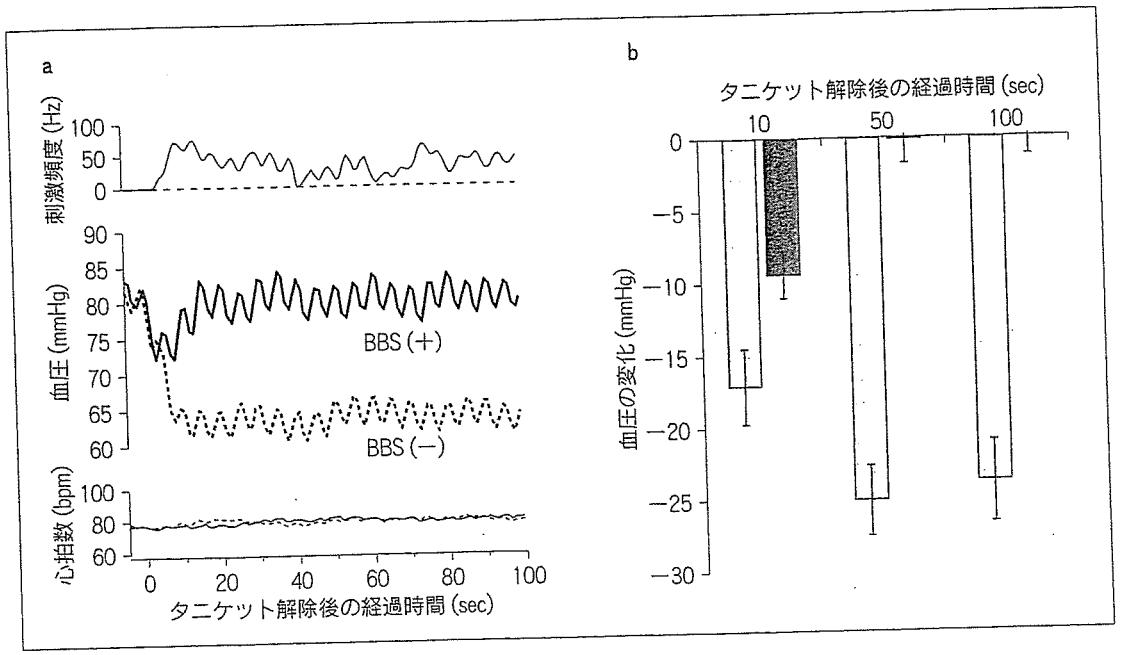

図6　バイオニック圧反射装置を用いた術中血圧制御

a：典型例．
b：21例における BBS の有効性に関する評価．BBS 未使用の場合（□）と BBS 使用の場合（▩）．数値は平均±標準偏差である．

また，脊髄交感神経刺激に対する血圧の応答特性を示す伝達関数を $H_2(f)$ とすると，被制御変数は次のように表される．

$$AP(f)=\frac{H_1(f)H_2(f)}{1+H_1(f)H_2(f)}AP_t(f)+\frac{1}{1+H_1(f)H_2(f)}AP_d(f)$$

ここで，$AP_d(f)$ は，サーボコントロールシステムに加わる外乱である．上の式から明らかなように，外乱の影響は，$1/(1+H_1(f)H_2(f))$ に抑制されることがわかる．

したがって，外乱に抗して血圧の安定化を図るためには，$H_1(f)$ の最適設計が必要である．そこで，まず，計測可能な $H_2(f)$ を次項のような方法で求め，ついで，数値シミュレーションにより $H_1(f)$ の係数 K_p および K_i を最適になるように設計した．

2.　サーボコントローラの設計

頸椎手術症例で，術中に脊髄誘発電位検査を施行予定の患者を対象にした．吸入麻酔薬による全身麻酔の導入後，経皮的に硬膜外カテーテル電極を挿入し，第9ないし第12胸椎レベルに電極を留置した．ついで刺激パルスのパラメータをパルス幅0.1ミリ秒，刺激頻度20 Hz に設定した．刺激強度は，この刺激パルスにより平均動脈圧がおおむね10 mmHg だけ上昇する電流値に調整した．筋弛緩薬投与下で，電気刺激装置に白色雑音様の不規則なトリガー信号を入力しながら，動脈圧の変動を15分間記録した．刺激パルスの頻度は，0 か 20 Hz かのいずれかになるように 8 秒間隔ごとに不規則に切り替えた．不規則刺激中の血圧応答の例を図 4a に，また推定された伝達関数 $H_2(f)$ を図 4b に示す．ついで，12例で求めた平均的 $H_2(f)$ を用いて，ステップ状の血圧低下（−20 mmHg）に対する血圧サーボシステムの振る舞いを比例補償係数 $K_p=0, 1, 2$，積分補償係数 $K_i=0, 0.01,$

0.05, 0.1, 0.2の組み合せでシミュレーションした．その結果，$K_p=1$, $K_i=0.1$の場合にもっとも迅速かつ安定的に血圧低下が防止されることが明らかとなった（図5）．そこで，$K_p=1$, $K_i=0.1$として人工的血管運動中枢をプログラムした．

3. BBSの有効性の検証

膝の人工関節置換術時に大腿に巻かれたタニケット（圧迫止血帯）の解除に伴う血圧低下を外乱とみなし，BBSの有効性を検証した．その結果，図6に示すように，BBSを用いることにより迅速で安全な自動血圧管理が可能であることが明らかになった[3]．

まとめ

神経インターフェイス技法に基づいたバイオニック療法が，慢性心不全に対する画期的な治療戦略となりうることを示す基礎研究結果，およびバイオニック圧反射装置により術中血圧を自動管理しうることを示唆する臨床研究結果を得ることができた．積極的に循環調節の破綻を是正したり，機能を再建することにより循環器疾患を治療するというバイオニック戦略の今後の展開に期待したい．

文献

1) Sato T, Kawada T, Sugimachi M et al: Bionic technology revitalizes native baroreflex function in rats with baroreflex failure. Circulation 2002; **106**: 730–734
2) Li M, Zheng C, Sato T et al: Vagal nerve stimulation markedly improves long-term survival after chronic heart failure in rats. Circulation 2004; **109**: 120–124
3) Yamasaki F, Ushida T, Yokoyama T et al: Artificial baroreflex: clinical application of a bionic baroreflex system. Circulation 2006; in press
4) Pfeffer MA: Left ventricular remodeling after acute myocardial infarction. Annu Rev Med 1995; **46**: 455–466
5) Cerati D, Schwartz PJ: Single cardiac vagal fiber activity, acute myocardial ischemia, and risk for sudden death. Circ Res 1991; **69**: 1389–1401
6) Schwartz PJ, La Rovere MT, Vanoli E: Autonomic nervous system and sudden cardiac death. Experimental basis and clinical observations for post-myocardial infarction risk stratification. Circulation 1992; **85** (Suppl I): I-77–I-91
7) La Rovere MT, Bigger JT Jr, Marcus FI et al: Baroreflex sensitivity and heart-rate variability in prediction of total cardiac mortality after myocardial infarction. Lancet 1998; **351**: 478–484
8) Lechat P, Hulot JS, Escolano S et al: Heart rate and cardiac rhythm relationships with bisoprolol benefit in chronic heart failure in CIBIS II trial. Circulation 2001; **103**: 1428–1433
9) Pfeffer MA, Pfeffer JM, Steinberg C et al: Survival after an experimental myocardial infarction: beneficial effects of long-term therapy with captopril. Circulation 1985; **72**: 406–412
10) Burkoff D, Sagawa K: Ventricular efficiency predicted by an analytic model. Am J Physiol 1986; **250**: R1021–R1027
11) Zhao G, Shen W, Xu X et al: Selective impairment of vagally mediated nitric oxide-dependent coronary vasodilation in conscious dogs after pacing-induced heart failure. Circulation 1995; **91**: 2655–2663
12) Kakinuma Y, Ando M, Kuwabara M et al: Acetylcholine from vagal stimulation protects cardiomyocytes against ischemia and hypoxia involving additive non-hypoxic induction of HIF-1α. FEBS Lett 2005; **579**: 2111–2118
13) Ando M, Katare RG, Kakinuma Y et al: Efferent vagal nerve stimulation protects heart against ischemia-induced arrhythmias by preserving connexin 43 protein. Circulation 2005; **112**: 164–170
14) Sato T, Kawada T, Inagaki M et al: New analytic framework for understanding sympathetic baroreflex control of arterial pressure. Am J Physiol 1999; **276**: H2251–H2261
15) Sato T, Kawada T, Shishido T et al: Novel therapeutic strategy against central baroreflex failure: a bionic baroreflex system. Circulation 1999; **100**: 299–304
16) Tanaka M, Nishikawa T: Arterial baroreflex function in humans anaesthetized with sevoflurane. Br J Anaesth 1999; **82**: 350–354
17) Keyl C, Schneider A, Hobbhahn J et al: Sinusoidal neck suction for evaluation of baroreflex sensitivity during desflurane and sevoflurane anesthesia. Anesth Analg 2002; **95**: 1629–1636
18) Tarkkila PJ, Kauknen S: Complications during spinal anesthesia: a prospective study. Reg Anesth 1991; **16**: 101–106

19) Kahn RL, Marino V, Urquhart B et al: Hemodynamic changes associated with tourniquet use under epidural anesthesia for total knee arthroplasty. Reg Anesth 1992; **17**: 228–232

20) Kawada K, Sunagawa G, Takaki H et al: Development of a servo-controller of heart rate using a treadmill. Jpn Circ J 1999; **63**: 945–950

REGULAR PAPER

J. Physiol. Sci. Vol. 56, No. 1; Feb. 2006; pp. 95–101
Online Feb. 25, 2006; **DOI: 10.2170/physiolsci.RP002305**

Nitric Oxide Stimulates Vascular Endothelial Growth Factor Production in Cardiomyocytes Involved in Angiogenesis

Masanori KUWABARA[1,2], Yoshihiko KAKINUMA[1], Motonori ANDO[1], Rajesh G. KATARE[1], Fumiyasu YAMASAKI[3], Yoshinori DOI[2], and Takayuki SATO[1]

[1]Department of Cardiovascular Control, Kochi Medical School, Nankoku, Japan; [2]Department of Medicine and Geriatrics, Kochi Medical School, Nankoku, Japan; and [3]Department of Clinical Laboratory, Kochi Medical School, Nankoku, Japan

Abstract: Background: Hypoxia-inducible factor (HIF)-1α regulates the transcription of lines of genes, including vascular endothelial growth factor (VEGF), a major gene responsible for angiogenesis. Several recent studies have demonstrated that a nonhypoxic pathway via nitric oxide (NO) is involved in the activation of HIF-1α. However, there is no direct evidence demonstrating the release of angiogenic factors by cardiomyocytes through the nonhypoxic induction pathway of HIF-1α in the heart. Therefore we assessed the effects of an NO donor, S-Nitroso-N-acetylpenicillamine (SNAP) on the induction of VEGF via HIF-1α under normoxia, using primary cultured rat cardiomyocytes (PRCMs). Methods and Results: PRCMs treated with acetylcholine (ACh) or SNAP exhibited a significant production of NO. SNAP activated the induction of HIF-1α protein expression in PRCMs during normoxia. Phosphatidylinositol 3-kinase (PI3K)–dependent Akt phosphorylation was induced by SNAP and was completely blocked by wortmannin, a PI3K inhibitor, and N^G-nitro-L-arginine methyl ester (L-NAME), a NO synthase inhibitor. The SNAP treatment also increased VEGF protein expression in PRCMs. Furthermore, conditioned medium derived from SNAP-treated cardiomyocytes phosphorylated the VEGF type–2 receptor (Flk-1) of human umbilical vein endothelial cells (a fourfold increase compared to the control group, $p < 0.001$, $n = 5$) and accelerated angiogenesis. Conclusion: Our results suggest that cardiomyocytes produce VEGF through a nonhypoxic HIF-1α induction pathway activated by NO, resulting in angiogenesis.

Key words: vascular endothelial growth factor, angiogenesis, cardiomyocyte, Flk-1, nitric oxide.

The prognosis of patients with chronic heart failure remains poor because of progressive remodeling of the heart and lethal arrhythmia [1]. It has recently been reported that vagal nerve stimulation therapy markedly improved long-term survival in an animal model of chronic heart failure after myocardial infarction [2] and that acetylcholine (ACh) has a direct cardioprotective effect through the PI3K-Akt-hypoxia-inducible factor (HIF)-1α pathway [3, 4]. Nitric oxide (NO) is supposed to be one of the signaling molecules induced by ACh; however, it remains to be clarified whether NO is involved in angiogenesis through the nonhypoxic induction pathway of HIF-1α and vascular endothelial growth factor (VEGF), and is thereby related to the cardioprotective effects of ACh or vagal nerve stimulation.

VEGF is a key angiogenic factor and major target of HIF-1α, which is produced by ischemic tissue and growing tumors [5–7]. Factors including VEGF secreted by noncardiomyocytes are known to possess significant paracrine effects on cardiomyocytes; however, the importance of such cardiomyocyte-derived factors as paracrine or autocrine effectors on angiogenesis in the heart remains to be elucidated. The HIF-1α protein level is usually regulated by the oxygen concentration. During hypoxia, HIF-1α protein is stabilized by escaping from degradation through von Hippel-Lindau tumor-suppressor protein (VHL) [8, 9]. Furthermore, the PI3K-Akt signaling pathway, which is known for the antiapoptotic functions [10, 11], is demonstrated to be involved in HIF-1α induction [12]. Recently it has been revealed that besides hypoxia, certain cytokines, growth factors, and NO increase the HIF-1α protein level even under the normoxic conditions in some specific cells [13–15]. To our knowledge, however, the involvement of NO in this signaling pathway in cardiomyocytes under normoxic conditions remains to be elucidated. Moreover, it is also unclear whether NO is involved in angiogenesis in the heart, though NO is associated with many aspects of cellular biology involved in cell signaling, vasodilatory tone, and cell growth [16].

With this background, we speculated the nonhypoxic induction of HIF-1α in the cardiomyocytes through NO-mediated pathway and that NO plays another role in producing an angiogenic factor through the pathway. To prove this hypothesis, we assessed the effect of a NO do-

Received on Dec 2, 2005; accepted on Feb 5, 2006; released online on Feb 25, 2006; DOI: 10.2170/physiolsci.RP002305
Correspondence should be addressed to: Yoshihiko Kakinuma, Department of Cardiovascular Control, Kochi Medical School, Nankoku, Kochi, 783-8505 Japan. Fax: +81-88-880-2310, Tel: +81-88-880-2587, E-mail: kakinuma@med.kochi-u.ac.jp

nor, *S*-Nitroso-*N*-acetylpenicillamine (SNAP), on the nonhypoxic induction of HIF-1α and the VEGF production in cardiomyocytes, using the primary cultured rat cardiomyocytes (PRCMs).

MATERIALS AND METHODS

Reagents. Reagents including the NO donor, *S*-nitroso-*N*-acetylpenicillamine (SNAP), acetylcholine (ACh), a phosphatidylinositol 3-kinase (PI3K) inhibitor, wortmannin, a specific nitric oxide synthase inhibitor, N^G-nitro-L-arginine methyl ester (L-NAME), and a transcriptional inhibitor, actinomycin D, were purchased from Sigma (Sigma Chemical Co., St. Louis, Missouri, USA).

Cell culture. This study followed the guidelines of the Council for Animal Care and was approved by an ethical committee of the Laboratory Animal Center, Kochi Medical School, Nankoku, Japan. According to the guideline, the Wistar rats used in this study were sacrificed. Primary cultured rat cardiomyocytes (PRCMs) were isolated from the hearts of 2-day-old neonatal rats and incubated on a gelatin-coated dish in DMEM/Ham F12 medium including 10% horse serum and ITS supplement according to our previous studies [17]. H9c2 cells have been frequently used to study the signal transductions and channels [18, 19]. H9c2 cells have been established as cell lines derived from the rat ventricular myocytes and thus far are widely used for many biological, biochemical, and electrophysiological studies because they have characteristics similar to PRCMs. Therefore they have often been utilized instead of PRCMs in studies where tons of rat cardiomyocytes are indispensable to perform experiments. To prepare many neonatal PRCMs for RNA isolation followed by RT-PCR, we used H9c2 cells, which, along with HEK 293, derived from human embryonic kidney cells, were incubated in DMEM supplemented with 10% FBS with antibiotics. To examine the effect of SNAP, cardiomyocytes in the serum-deficient medium were treated with either 1 μM (PRCMs, HEK 293 cells) or 1 mM (H9c2 cells) of SNAP.

Determination of NO from cardiomyocytes. To determine whether ACh and SNAP release NO in cardiomyocytes, we used an NO-sensitive fluorescent dye, diaminofluorescein-2 (DAF-2) (Daiichi Pure Chemicals Co. Ltd., Tokyo, Japan) [20]. PRCMs were treated with 10 μM DAF-2 and 100 μM L-arginine for 60 min, followed by 1 μM SNAP or 1 mM ACh. To examine the effect of L-NAME on NO production, the PRCMs were first pretreated with 1 mM L-NAME for 60 min, followed by the addition of DAF-2 and L-arginine. After incubation at 37°C, the cells were washed with PBS and observed under a fluorescence microscopy.

Western blotting analysis. To investigate the signal transduction pathway from SNAP to VEGF, we evaluated the effect of wortmannin (30 nM), actinomycin D (0.5 μg/ml), and L-NAME (1 mM) on Akt, HIF-1α, and VEGF by immunoblotting assay [21, 22]. Cardiomyocytes were pretreated with one of these agents prior to the addition of SNAP. After the incubation with SNAP, the cells were lysed and the total proteins isolated. The samples were then fractionated by 10% SDS-PAGE and transferred onto a PVDF membrane. Immunoblotting was performed with the primary antibodies against HIF-1α, VEGF (Santa Cruz Biotechnology, Santa Cruz, California, USA), Akt, phospho-Akt (Cell Signaling Technology, Beverly, Massachusetts, USA), or tubulin-α (Lab Vision, Fremont, California, USA), and was then reacted with an appropriate HRP-conjugated secondary antibody. The signal was detected with an enhanced chemiluminescence system (ECL Plus, Amersham, Piscataway, New Jersey, USA). Each experiment was performed in a duplicated fashion and repeated five times (n = 5), and representative data were shown.

Transfection. To investigate the direct contribution of HIF-1α to VEGF expression, HEK 293 cells were transfected with an expression vector for dominant-negative HIF-1α (dn HIF-1α) [23], using Effectene (Qiagen, Valencia, CA, USA) according to the manufacturer's protocol. HEK293 cells are derived from human embryonic kidney cells. It is known that the transient transfection of PRCMs with a conventional method is difficult and that the efficacy is extremely low. Compared with PRCMs, HEK293 cells have been extensively used for the transient transfection of an interested gene because of the extremely high efficiency of transfection and the higher protein expression level. Therefore we used HEK293 cells. Thirty-six hours after transfection, the HEK 293 cells were pretreated with 1 μM SNAP for 12 h, followed by an evaluation of the VEGF protein level. As a control, the cells were transfected with a vector for green fluorescent protein (GFP).

Reverse transcription-PCR (RT-PCR). RNA isolation and RT-PCR were performed as described earlier [17]. The synthesized cDNA was amplified with gene-specific primers for HIF-1α, VEGF, and Glut-1, as well as β-actin. The sense and antisense gene-specific primers were as follows:

HIF-1α (sense), 5'-GGGAGAAAAGCAAGTCGTG-3',
HIF-1α (antisense), 5'-AGTCAGCAACGTGGAAGG-3';
VEGF (sense), 5'-CCAGCACATAGGAGAGATGAGCTTC-3',
VEGF (antisense), 5'-GGTGTGGTGGTGACATGGTTAATC-3';
Glut-1 (sense), 5'-ACACCTCCCCCACATACATG-3',
Glut-1 (antisense), 5'-TGGAGTTTGGCTATAACACC-3';
β-actin (sense), 5'-GAAGATCCTGACCGAGCGTG-3',
β-actin (antisense), 5'-CGTACTCCTGCTTGCTGATCC-3'.

The optimal annealing temperature and the number of cycles for each template is as follows: 54°C, 30 cycles for HIF-1α; 62°C, 34 cycles for VEGF; 62°C, 36 cycles for Glut-1; and 60°C, 32 cycles for β-actin. PCR was performed in the range that gave a linear correlation between the amount of cDNA and the yield of PCR products. The

ratio of the RT-PCR product for each gene to that of β-actin was quantified and compared.

Immunohistochemistry. After SNAP treatment, H9c2 cells were fixed with 4% paraformaldehyde for 10 min and treated with 1% Triton X-100 for another 10 min. To block nonspecific antibody binding, the cells were incubated with 5% skim milk and successively incubated with a VEGF antibody (Santa Cruz Biotechnology, Santa Cruz, California, USA) in 1% skim milk at 4°C overnight and an FITC-labeled secondary antibody (Jackson ImmunoResearch Laboratories, West Grove, PA, USA) at 4°C overnight, then examined with an immunofluorescence microscope.

Human umbilical vein endothelial cells (HUVECs) culture. To understand if NO induces the cardiomyocytes to produce a factor responsible for angiogenesis, we examined the effect of conditioned medium derived from H9c2 cells treated with SNAP on HUVECs. The HUVECs were cultured in EGM-2 culture medium supplemented with angiogenic and growth factors (Cambrex Bio Science Walkersville, Inc., Walkersville, Maryland, USA). The H9c2 cells were treated with SNAP for 2 h and then incubated in the serum-free fresh medium. After 10 hours, the supernatant was collected and added to the HUVECs by replacing EGM-2 medium. The samples were collected before and after 60 min of stimulation with conditioned medium to evaluate the phosphorylation of VEGF receptor (Flk-1), using anti–pFlk-1 antibody (Santa Cruz Biotechnology, Santa Cruz, California, USA).

To further investigate the angiogenic effect of the conditioned medium derived from cardiomyocytes, the HUVECs were cultured on Matrigel (Becton Dickinson Labware, Bedford, Maryland, USA). The 96-well plates were coated with the diluted Matrigel (50 μl/well), incubated at 37°C for 1 h, then washed with serum-free DMEM. The HUVECs (1×10^4 cells) were seeded onto each well and cultured at 37°C for 10 h in DMEM, supplemented with 20% FBS, 25 μg/ml endothelial cell growth supplement (ECGS), 10 U/ml heparin, and conditioned medium derived from SNAP-treated or nontreated H9c2 cells.

Statistical analysis. Data are presented as mean ± SE. The differences were assessed by ANOVA followed by Fisher's PLSD for multiple comparisons. The results were considered statistically significant at $p < 0.05$.

RESULTS

A nonhypoxic induction of HIF-1α by NO through PI3K-Akt pathway

ACh or SNAP treatment rapidly increased the NO release in PRCMs within 30 min (Fig. 1); the release was continued and peaked at 8 h. In contrast, the cells pretreated with a nitric oxide synthase inhibitor L-NAME (1 mM) failed to show the NO signal (Fig. 1). The HIF-1α protein

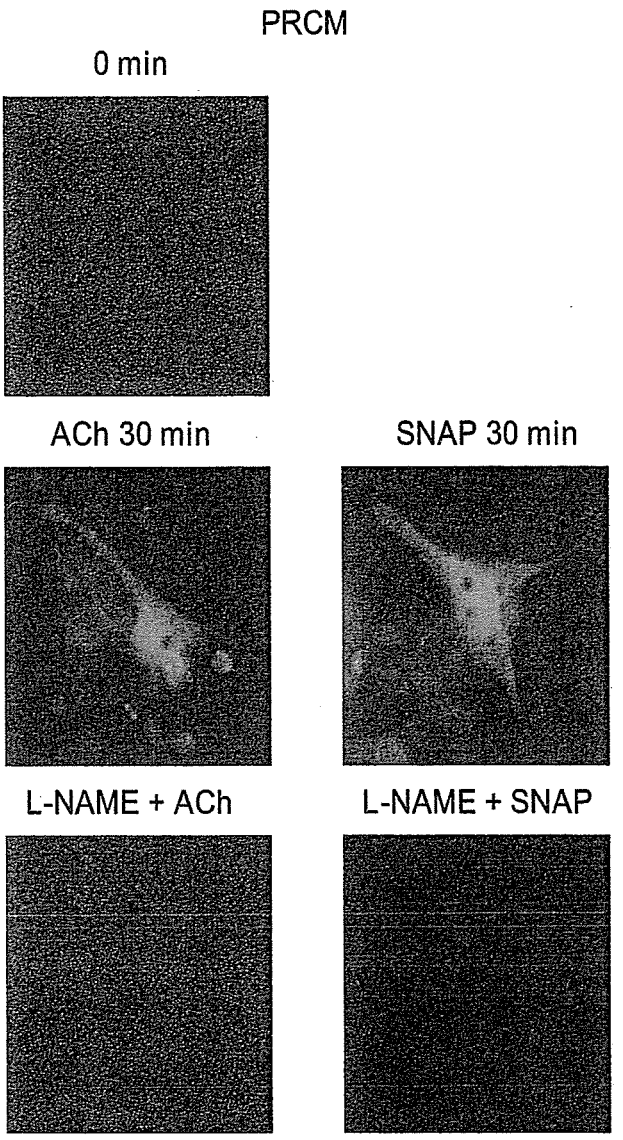

Fig. 1. Rat primary cardiomyocytes release NO in response to ACh or SNAP. PRCMs released NO after treatment with 1 mM ACh or 1 μM SNAP, evaluated with DAF-2. NO release was observed within 30 min after ACh or SNAP treatment ($n = 3$). Pretreatment with 1 mM L-NAME for 60 min blocked NO production ($n = 3$).

expression was gradually increased within 8 h since the SNAP treatment (a fivefold increase compared to the baseline (0 h), $p < 0.001$, $n = 5$) in PRCMs under normoxic conditions, thus confirming the occurrence of a nonhypoxic pathway for the HIF-1α induction in the cardiomyocytes (Fig. 2a). Such an induction of HIF-1α was also observed in H9c2 cells (data not shown). To understand if this induction is regulated at the transcriptional level, we pretreated cardiomyocytes with a commonly used transcriptional inhibitor, actinomycin D (0.5 μg/ml), followed by stimulation with SNAP for 8 h. However, actinomycin D failed to inhibit the HIF-1α induction by SNAP (Fig.

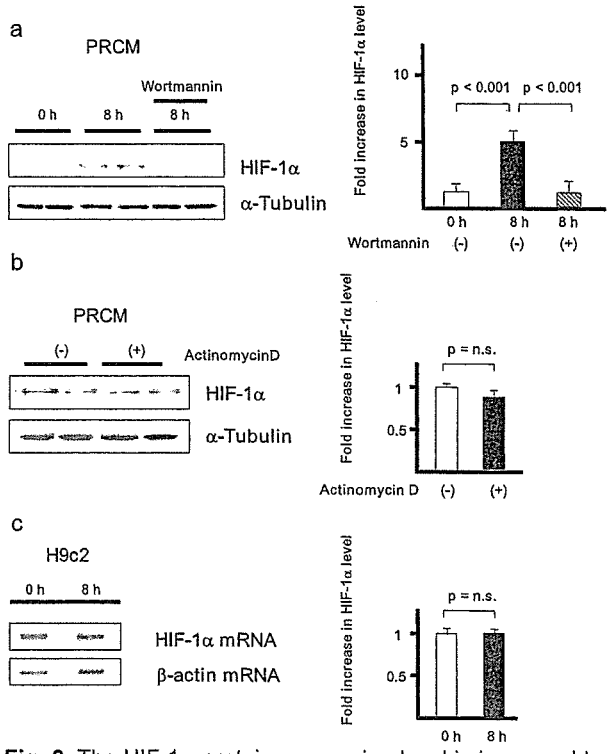

Fig. 2. The HIF-1α protein expression level is increased by SNAP in cardiomyocytes in normoxia. Treating the PRCMs for 8 h with SNAP (1 μM) already increased HIF-1α protein expression in normoxia. Pretreatment of PRCMs with wortmannin (30 nM) for 30 min inhibited SNAP-induced HIF-1α expression ($n = 5$) (**a**). However, treatment with actinomycin D (0.5 μg/ml) for 15 min did not inhibit the upregulation of HIF-1α protein expression by SNAP ($n = 5$) (**b**). In H9c2 cells, the HIF-1α mRNA expression level was not increased by SNAP ($n = 5$) (**c**).

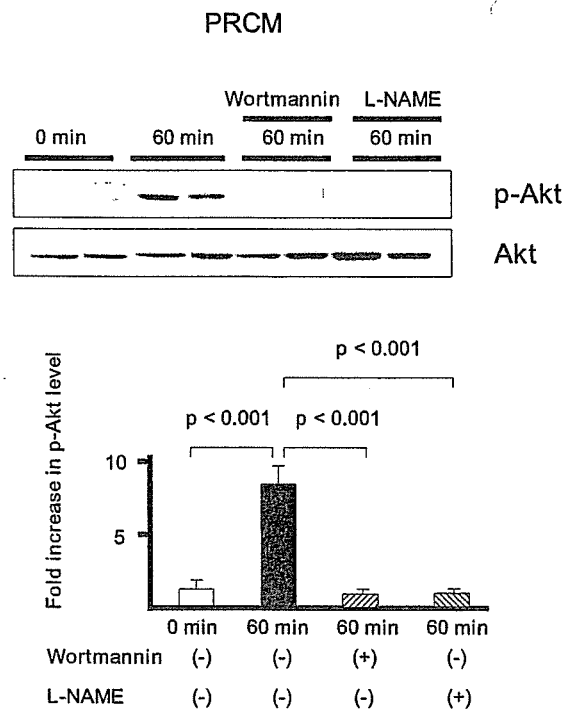

Fig. 3. Akt phosphorylation is increased by SNAP in cardiomyocytes under normoxia. Akt phosphorylation was increased by SNAP (1 μM) in PRCMs with a rapid time course. However, pretreatment with wortmannin (30 nM) for 60 min or L-NAME (1 mM) for 60 min completely inhibited the Akt phosphorylation in cardiomyocytes ($n = 5$).

2b), and SNAP further did not increase the HIF-1α mRNA level, evaluated by RT-PCR (Fig. 2c), thus suggesting that SNAP induces HIF-1α posttranslationally in normoxic conditions. Western blotting analysis further revealed an increased Akt phosphorylation with SNAP treatment for 60 min compared to the baseline (0 min) (an eightfold increase from the baseline, $p < 0.001$, $n = 5$) in PRCMs (Fig. 3). Pretreating the cells with PI3K inhibitor wortmannin (30 nM) or nitric oxide synthase inhibitor L-NAME (1 mM) prevented the SNAP-induced Akt phosphorylation (Fig. 3), thus demonstrating an important role for PI3K and NO in the Akt signaling pathway. Even though wortmannin (30 nM) was able to inhibit the SNAP-induced Akt or HIF-1α induction, it failed to block the NO release by the SNAP-treated cardiomyocytes (data not shown), thus confirming that NO remains upstream to the PI3K-Akt pathway. Moreover, these results also suggest the NO-dependent induction of HIF-1α in the cardiomyocytes under normoxic conditions.

Promotion of angiogenic signaling cascade by NO in cardiomyocytes under normoxia

To identify if SNAP-induced HIF-1α actually affects transcriptional activation of the target genes, the gene expression levels of the Glut-1 and VEGF were evaluated by the use of RT-PCR. The treatment of H9c2 cells with SNAP for 12 h under normoxic conditions increased the gene expressions of Glut-1 and VEGF, major HIF-1α–regulated genes (Fig. 4a). The protein expression level of VEGF was also increased following SNAP treatment, as demonstrated by the immunohistochemical and Western blotting analysis (Fig. 4 b and c). Consistent with the earlier findings, wortmannin was also able to inhibit the SNAP-induced VEGF expression in H9c2 cells and PRCMs (Fig. 4c), thus suggesting the PI3K-Akt mediated HIF-1α induction pathway in the production of VEGF by the cardiomyocytes under normoxic conditions. Furthermore, to elucidate the contribution of HIF-1α to VEGF protein expression, dn HIF-1α was introduced into HEK293 cells, and it was demonstrated that dn HIF-1α partially inhibits the VEGF induction by SNAP (Fig. 4d).

VEGF production in cardiomyocytes was further confirmed by an addition of conditioned medium derived from SNAP-treated or nontreated H9c2 cells to the HUVECs. As expected, the conditioned medium-treated cells

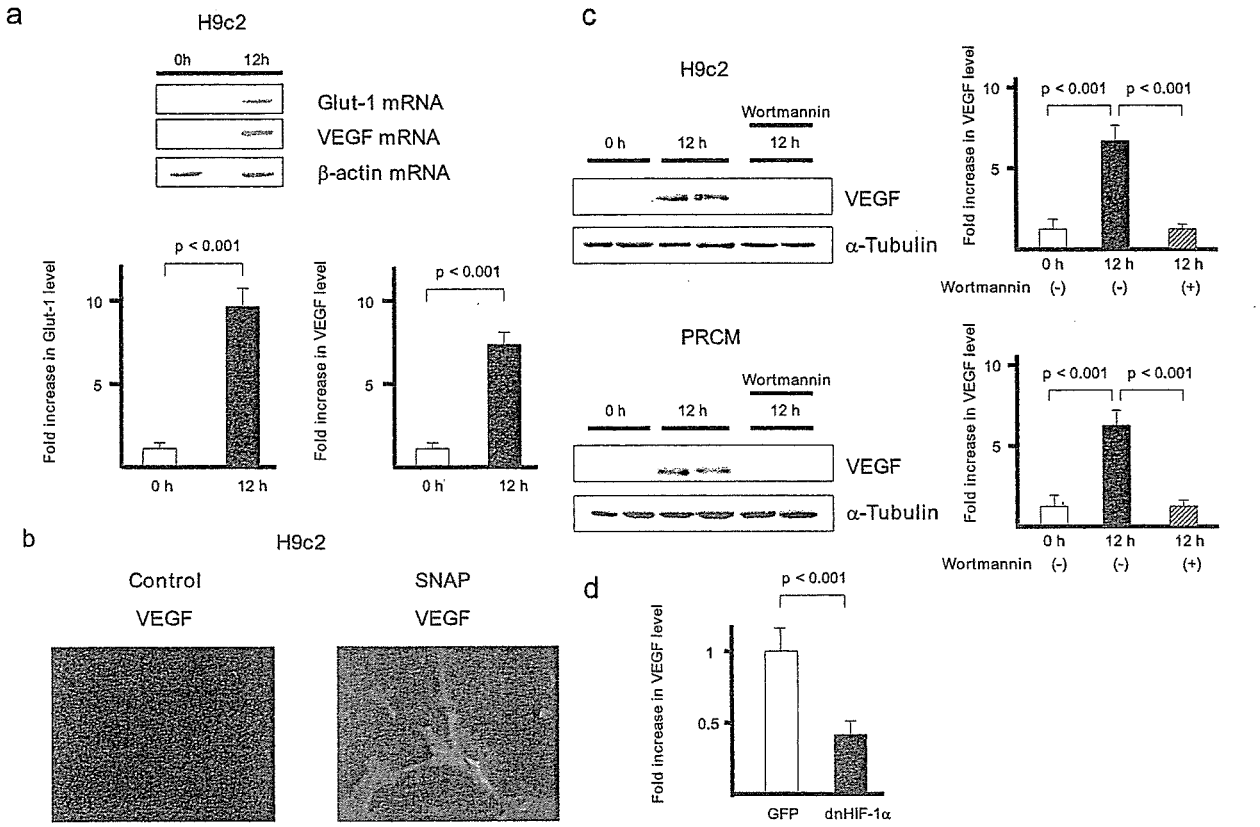

Fig. 4. SNAP increases Glut-1 and VEGF gene expression levels through HIF-1α in cardiomyocytes under normoxia. In H9c2 cells, Glut-1 mRNA and VEGF mRNA were both increased by SNAP (n = 5) (**a**). VEGF immunoreactivity was increased by SNAP in H9c2 cells (n = 5) (**b**). The SNAP-induced VEGF protein expression, which was also observed in PRCMs, was completely inhibited by 30 nM wortmannin (n = 5) (**c**). In contrast to control (GFP), VEGF induction by SNAP was blocked by dn HIF-1α in HEK293 cells (n = 5) (**d**).

(SNAP group) revealed increased Flk-1 phosphorylation (a fourfold increase compared to the control group, $p < 0.001$, $n = 5$), a VEGF type-2 receptor responsible for angiogenesis, in HUVECs (Fig. 5a). Furthermore, HUVECs were cultured on Matrigel in the presence of conditioned medium. Compared with the control group, the SNAP group activated more angiogenesis. It is suggested that SNAP exerts an acceleration of angiogenesis partially via cardiomyocyte-derived angiogenic factors, including VEGF (Fig. 5b).

DISCUSSION

It is well known that NO plays a critical role in modulating the vascular tone. According to the vascular effect, the depressed functional capacity of NO production would result in vasoconstriction and poor collateral circulation. Therefore NO or a NO donor has been used for coronary vasodilatation and decreasing blood pressure in systemic or pulmonary hypertension. However, the other effect of NO or a NO donor on cardiomyocytes remains to be fully investigated. It is known that NO is synthesized through eNOS in endothelial cells, and it is speculated that it has a significant paracrine effect on cardiomyocytes; however, it is unclear whether cardiomyocyte-derived NO possesses the direct action on cardiomyocytes to produce angiogenic factors.

Our previous study demonstrated the involvement of PI3K-Akt pathway in inducing the expression of HIF-1α by ACh during normoxia [4]. In the present study, SNAP-treated cardiomyocytes revealed a similar pathway in the induction of HIF-1α, suggesting that NO from cardiomyocytes activates an angiogenic signaling through HIF-1α.

As shown in the present study using DAF-2, a NO-sensitive dye, NO was detected in cardiomyocytes in response to SNAP as well as ACh, suggesting that cardiomyocytes release NO. The NO release by SNAP appeared in a rapid time course 30 min after the treatment, and it was not detected in PRCMs pretreated with L-NAME. Other studies have also reported the inhibitory effects of L-NAME on SNAP without the exact mechanisms being identified [24–27]; however, the speculated mechanism could be that the L-NAME pretreatment for 60 min of PRCMs might inhibit NO synthase, thereby reducing the basal NO production. Even if SNAP was thereafter added for 30 min to enhance NO release, the NO level in

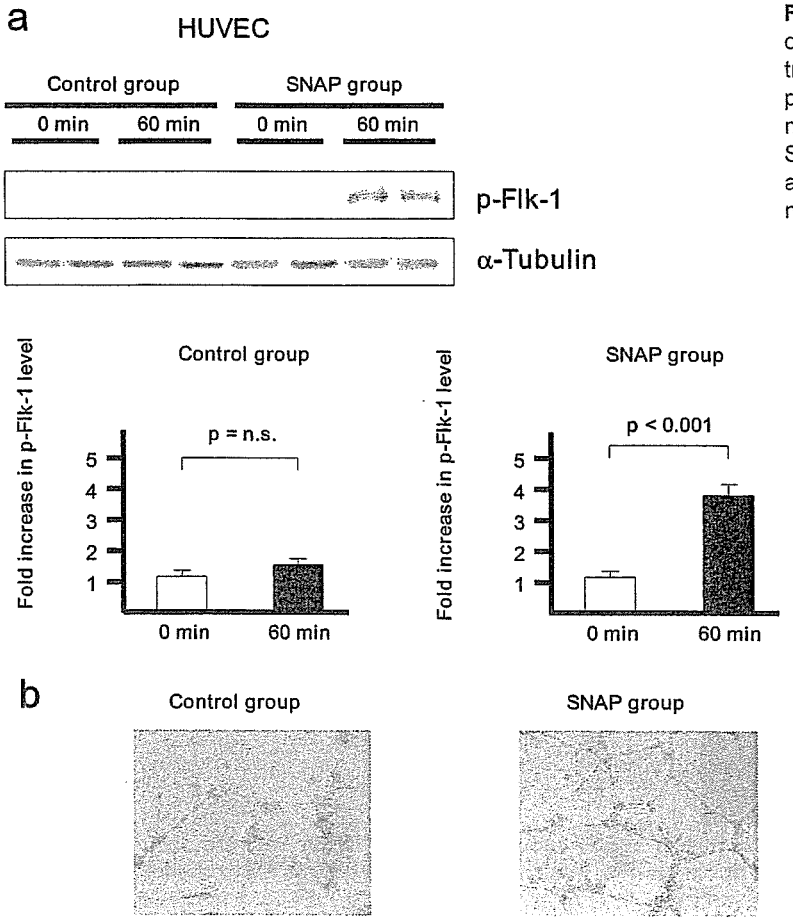

Fig. 5. VEGF derived from SNAP-treated cardiomyocytes induces angiogenesis. The SNAP-treated conditioned medium increased Flk-1 phosphorylation in HUVECs, compared with the nontreated conditioned medium (n = 5) (**a**). The SNAP-treated conditioned medium accelerated angiogenesis in HUVECs compared with the nontreated conditioned medium (**b**).

the treated cardiomyocyte might be too low, compared with the nontreated cell, to be detected by DAF-2. Therefore, these results suggest that cardiomyocyte-derived NO as a paracrine or autocrine effector plays a critical role in the HIF-1α induction in cardiomyocytes.

Second, as shown in this study, NO increased the cardiac VEGF protein expression through HIF-1α regulation, and dn HIF-1α decreased the VEGF expression by SNAP. VEGF itself has been reported to be involved in cell survival through the tyrosine kinase receptors, including VEGF type-2 receptor (Flk-1), activating Akt via a PI3K-dependent pathway [28], leading to eNOS upregulation. Furthermore, as suggested in our study, the cardiomyocyte-derived VEGF plays a crucial role in accelerating angiogenesis by endothelial cells in a paracrine fashion because VEGF produced by cardiomyocytes phosphorylated Flk-1 in HUVECs. These results suggest that cardiomyocytes can not only be a target for a NO donor to activate a nonhypoxic pathway of HIF-1α, but can also play a role in producing angiogenic factors in the heart. Taken together, the beneficial effects of NO might in part be a result of the cell signaling through PI3K-Akt, and also in part a result of the angiogenic signaling through HIF-1α–VEGF.

In the recent study by Giordano *et al.* [29], a cardiomyocyte-specific knockout of VEGF caused impaired cardiac development with hypovascularity in the heart, suggesting that cardiomyocyte-induced VEGF production is essential for cardiac development; however, their study did not reveal the precise cellular mechanism by which cardiac VEGF deletion leads to hypovasculature and depressed cardiac function. Our present study indicated that HIF-1α induction through NO plays a main role in stimulating VEGF production by cardiomyocytes and accelerates angiogenesis.

In this study we focused on HIF-1α as an upstream factor regulating cardiac VEGF expression. Unlike the hypoxic induction pathway of HIF-1α, there is no direct evidence for a nonhypoxic induction pathway of cardiomyocytes through NO involved in angiogenesis. Consequently, this study revealed another pathway of cardiac HIF-1α induction. PI3K-Akt signal has many aspects in cell survival, including an antiapoptotic activity, such as an inhibition of Bad-binding to Bcl-2 through Akt phosphorylation, an inhibition of proapoptotic caspases, including caspase 9 and Fas, and an inhibition of the activity of proapoptotic glycogen synthetase kinase-3 [30, 31]. In previous studies, which used other cell lines, the PI3K-

Akt pathway has been demonstrated to be involved in the NO-dependent stabilization of HIF-1α [14, 32–34]. As demonstrated in this study, in the presence of actinomycin D, the dose of which is adequate to inhibit transcriptional activity, SNAP posttranslationally regulated HIF-1α. Actinomycin D was used to identify which mechanisms are responsible for the increased protein expression, i.e., de novo synthesis or posttranslational modification. The protein level of HIF-1α was not decreased by actinomycin D; therefore this suggests that SNAP does not play a role in the transcriptional regulation of HIF-1α, rather in the inhibition of protein degradation. Therefore in cardiomyocytes, such a mechanism might be involved in a NO-mediated Akt-HIF-1α-VEGF signaling pathway, leading to cell protection.

In conclusion, it is suggested that NO has beneficial effects on cardiomyocytes by the activation of the nonhypoxic HIF-1α induction pathway, and furthermore, it contributes to angiogenesis through cardiac VEGF production, which phosphorylates Flk-1, a VEGF type-2 receptor.

This study was supported by a Health and Labor Sciences Research Grant (H15-PHYSI-001) for Advanced Medical Technology from the Ministry of Health, Labor, and Welfare of Japan.

REFERENCES

1. Julian DG, Gamm AJ, Frangin G, Janse MJ, Munoz A, Schwartz PJ, Simon P. Randomised trial of effect of amiodarone on mortality in patients with left-ventricular dysfunction after recent myocardial infarction: EMIAT. European Myocardial Infarct Amiodarone Trial Investigators. Lancet. 1997;349:667-74.
2. Li M, Zheng C, Sato T, Kawada T, Sugimachi M, Sunagawa K. Vagal nerve stimulation markedly improves long-term survival after chronic heart failure in rats. Circulation. 2004;109:120-4.
3. Krieg T, Qin Q, Philipp S, Alexeyev MF, Cohen MV, Downey JM. Acetylcholine and bradykinin trigger preconditioning in the heart through a pathway that includes Akt and NOS. Am J Physiol Heart Circ Physiol. 2004;287:H2606-11.
4. Kakinuma Y, Ando M, Kuwabara M, Rajesh G, Okudela K, Kobayashi M, Sato T. Acetylcholine from vagal stimulation protects cardiomyocytes against ischemic and hypoxia involving additive non-hypoxic condition of HIF-1α. FEBS Lett. 2005;579:2111-8.
5. Semenza GL. Hypoxia-inducible factor 1. oxygen homeostasis and disease pathophysiology. Trends Mol Med. 2001;7:345-50.
6. Ferrara N, Houck K, Jakeman L, Leung DW. Molecular and biological properties of the vascular endothelial growth factor family of proteins. Endocr Rev. 1992;13:18-32.
7. Wang GL, Jiang BH, Rue EA, Semenza GL. Hypoxia-inducible factor 1 is a basic-helix-loop-helix-PAS heterodimer regulated by cellular O_2 tension. Proc Natl Acad Sci USA. 1995;92:5510-4.
8. Maxwell PH, Wiesener MS, Chang GW, Clifford SC, Vaux EC, Cockman ME, Wykoff CC, Pugh CW, Maher ER, Ratcliffe PJ. The tumour suppressor protein VHL targets hypoxia-inducible factors for oxygen-dependent proteolysis. Nature. 1999;399:271-5.
9. Ivan M, Kondo K, Yang H, Kim W, Valiando J, Ohh M, Salic A, Asara JM, Lane WS, Kaelin Jr WG. HIF-1α targeted for VHL-mediated destruction by proline hydroxylation: Implications for O_2 sensing. Science. 2001;292:464-8.
10. Cantley LC, Auger KR, Carpenter C, Duckworth B, Graziani A, Kapeller R, Soltoff S. Oncogenes and signal transduction. Cell. 1991;64:281-302.
11. Yao R, Cooper GM. Requierment for phosphatidylinositol-3 kinase in the prevention of apoptosis by nerve growth factor. Science. 1995;267:2003-6.
12. Kandel ES, Hay N. The regulation and activities of the multifunctional serine/threonine kinase Akt/PKB. Exp Cell Res. 1999;253:210-29.
13. Richard DE, Berra E, Pouysségur J. Nonhypoxic pathway mediates the induction of hypoxia-inducible factor 1α in vascular smooth muscle cells. J Biol Chem. 2000;275:26765-71.
14. Sandau KB, Zhou J, Kietzmann T, Brune B. Regulation of the hypoxia-inducible factor 1 alpha by the inflammatory mediators nitric oxide and tumor necrosis factor-alpha in contrast to desferroxamine and phenylarsine oxide. J Biol Chem. 2001;276:39805-11.
15. Sandau KB, Fandrey J, Brune B. Accumulation of HIF-1alpha under the influence of nitric oxide. Blood. 2001;97:1009-15.
16. Balligand JL, Cannon PJ. Nitric oxide synthases and cardiac muscle: Autocrine and paracrine influences. Arterioscler Thromb Vasc Biol. 1997;17:1846-58.
17. Kakinuma Y, Miyauchi T, Yuki K, Murakoshi M, Goto K, Yamaguchi I. Novel molecular mechanism of increased myocardial endothelin-1 expression in the failing heart involving the transcriptional factor HIF-1α induced for impaired myocardial energy metabolism. Circulation. 2001; 103:2387-4.
18. Ilangovan G, Osinbowale S, Bratasz A, Bonar M, Cardounel AJ, Zweier JL, Kuppusamy P. Heat shock regulates the respiration of cardiac H9c2 cells through upregulation of nitric oxide synthase. Am J Physiol Cell Physiol. 2004;287:C1472-81.
19. Wu G, Mannam AP, Wu J, Kirbis S, Shie JL, Chen C, Laham RJ, Sellke FW, Li J. Hypoxia induces myocyte-dependent COX-2 regulation in endothelial cells: role of VEGF. Am J Physiol Heart Circ Physiol. 2003;285:H2420-H9.
20. Kimura C, Koyama T, Oike M, Ito Y. Hypotonic stress-induced NO production in endothelium depends on endogenous ATP. Biochem Biophys Res Commun. 2000;274:736-40.
21. Chachami G, Simos G, Hatziefthimiou A, Bonanou S, Molyvdas PA, Paraskeva E. Cobalt induces hypoxia-inducible factor-1alpha expression in airway smooth muscle cells by a reactive oxygen species and PI3K-dependent mechanism. Am J Respir Cell Mol Biol. 2004;31:544-51.
22. Weller R, Schwentker A, Billiar TR, Vodovotz Y. Autologous nitric oxide protects mouse and human keratinocytes from ultraviolet B radiation-induced apoptosis. Am J Physiol Cell Physiol. 2003;284:C1140-8.
23. Chen J, Zhao S, Nakada K, Kuge Y, Tamaki N, Okada F, Wang J, Shindo M, Higashino F, Takeda K, Asaka M, Katoh H, Sugiyama T, Hosokawa M, Kobayashi M. Dominant-negative hypoxia-inducible factor-1 alpha reduces tumorigenicity of pancreatic cancer cells through the suppression of glucose metabolism. Am J Pathol. 2004;162:1283-91.
24. Dang VC *et al.* Nitric oxide-cGMP-protein kinase G signaling pathway induces anoxic preconditioning through activation of ATP-sensitive K^+ channels in rat hearts. Am J Physiol Heart Circ Physiol. (Epub) Dec 9. 2005.
25. Chen J, Zhu JX, Wilson I, Cameron JS. Cardioprotective effects of K_{ATP} channel activation during hypoxia in goldfish carassius auratus. J Exp Biol. 2005;208:2765-72.
26. Maejima Y *et al.* Nitric oxide inhibits ischemia/reperfusion-induced myocardial apoptosis by modulating cyclin A-associated kinase activity. Cardiovasc Res. 2003;59:308-20.
27. Ebihara Y *et al.* Modulation of endothelin-a effects on rat hearts and cardiomyocytes by nitric oxide and 8-bromo cyclic GMP. J Mol Cell Cardiol. 1996;28:265-77.
29. Gerber HP, McMurtrey A, Kowalski J, Yan M, Kety BA, Dixit V, Ferrara N. Vascular endothelial growth factor regulates endothelial cell survival through the phosphatidyl-inositol 3'-kinase/Akt signal transduction pathway. Requirement for Flk-1/KDR activation. J Biol Chem. 1998;273:30336-43.
29. Giordano FJ, Gerber HP, Williams SP, VanBruggen N, Bunting S, Ruiz-Lozano P, Gu Y, Nath AK, Huang Y, Hickey R, Dalton N, Peterson KL, Ross J Jr, Chien KR, Ferrara N. A cardiac myocyte vascular endothelial growth factor paracrine pathway is required to maintain cardiac function. Proc Natl Acad Sci USA. 2001;98:5780-5.
30. Kennedy SG, Wagner AJ, Conzen SD, Jordan J, Bellacosa A, Tsichlis PN, Hay N. The PI3-kinase/Akt signaling pathway delivers an anti-apoptotic signal. Genes Dev. 1997;11:701-13.
31. Cross DA, Alessi DR, Cohen P, Andjelkovich M, Hemmings BA. Inhibition of glycogen synthase kinase-3 by insulin mediated by protein kinase B. Nature. 1995;378:785-9.
32. Kasuno K, Takabuchi S, Fukuda K, Kizaka-Kondoh S, Yodoi J, Adachi T, Semenza GL, Hirota K. Nitric oxide induces hypoxia-inducible factor 1 activation that is dependent on MAPK and phosphatidylinositol 3-kinase signaling. J Biol Chem. 2004;279:2550-8.
33. Sandau KB, Faus HG, Brune B. Induction of hypoxia-inducible-factor 1 by nitric oxide is mediated via the PI3K pathway. Biochem Biophys Res Commun. 2000;278:263-7.
34. Matzen E, Zhou J, Jelkmann W, Fandrey J, Brune B. Nitric oxide impairs normoxic degradation of HIF-1α by inhibition of prolyl hydroxylases. Mol Biol Cell. 2003;14:3470-81.

Artificial Baroreflex

Clinical Application of a Bionic Baroreflex System

Fumiyasu Yamasaki, MD; Takahiro Ushida, MD; Takeshi Yokoyama, DDS; Motonori Ando, PhD; Koichi Yamashita, MD; Takayuki Sato, MD

Background—We proposed a novel therapeutic strategy against central baroreflex failure: implementation of an artificial baroreflex system to automatically regulate sympathetic vasomotor tone, ie, a bionic baroreflex system (BBS), and we tested its efficacy in a model of sudden hypotension during surgery.

Methods and Results—The BBS consisted of a computer-controlled negative-feedback circuit that sensed arterial pressure (AP) and automatically computed the frequency (STM) of a pulse train required to stimulate sympathetic nerves via an epidural catheter placed at the level of the lower thoracic spinal cord. An operation rule was subsequently designed for the BBS using a feedback correction with proportional and integral gain factors. The transfer function from STM to AP was identified by a white noise system identification method in 12 sevoflurane-anesthetized patients undergoing orthopedic surgery involving the cervical vertebrae, and the feedback correction factors were determined with a numerical simulation to enable the BBS to quickly and stably attenuate an external disturbance on AP. The performance of the designed BBS was then examined in a model of orthostatic hypotension during knee joint surgery (n=21). Without the implementation of the BBS, a sudden deflation of a thigh tourniquet resulted in a 17±3 mm Hg decrease in AP within 10 seconds and a 25±2 mm Hg decrease in AP within 50 seconds. By contrast, during real-time execution of the BBS, the decrease in AP was 9±2 mm Hg at 10 seconds and 1±2 mm Hg at 50 seconds after the deflation.

Conclusions—These results suggest the feasibility of a BBS approach for central baroreflex failure. (***Circulation*. 2006; 113:634-639.**)

Key Words: baroreceptors ■ blood pressure ■ computers ■ electrical stimulation ■ nervous system, sympathetic

The arterial baroreflex acts to maintain cerebral perfusion by quickly attenuating the effect of an external disturbance, such as the assumption of an upright position, on arterial pressure (AP).[1–4] Therefore, functional restoration of dynamic properties of the arterial baroreflex is essential for the treatment of patients with various syndromes of baroreflex failure,[5] including Shy-Drager syndrome,[6–9] baroreceptor deafferentation,[10,11] and traumatic spinal cord injuries.[12,13] However, most commonly used interventions, including salt loading,[14,15] cardiac pacing,[16,17] and adrenergic agonists,[18,19] can neither restore nor reproduce the functioning of the native vasomotor center, and most affected patients remain bedridden.

Clinical Perspective p 639

We recently developed a framework for identifying an operational rule of the vasomotor center and a prototype of a bionic baroreflex system (BBS) in rats.[20–22] The BBS consisted of a negative-feedback system controlled by a computer (ie, the artificial vasomotor center) that sensed AP and automatically computed the frequency of a pulse train required to stimulate sympathetic efferent nerves through a pair of wire electrodes placed in the celiac ganglion. Previous experimental work demonstrated that the BBS restored native baroreflex function in rats with central baroreflex failure; however, an applicable neural interface with quick and effective controllability of AP is required for application of this technology in the clinical setting. The goal of the present study was to determine the efficacy of a novel bionic technology for the intraoperative restoration of AP in the context of central baroreflex failure and to validate this technology in a clinical model of orthostatic hypotension.

Methods

All studies were approved by the institutional review committee, and all subjects gave informed consent.

Theoretical Considerations

As previously described,[20–22] the principle of the BBS is based on a negative-feedback mechanism (Figure 1). The instantaneous AP is measured by a pressure transducer connected to a computer that functions as a controller or artificial vasomotor center. Instead of the disabled native vasomotor center, the controller automatically exe-

Received September 8, 2005; revision received October 31, 2005; accepted November 21, 2005.

From the Departments of Cardiovascular Control (F.Y., M.A., T.S.), Clinical Laboratory (F.Y.), Orthopedic Surgery (T.U.), and Anesthesiology (T.Y., K.Y.), Kochi Medical School, Nankoku, Japan.

Correspondence to Fumiyasu Yamasaki, MD, Department of Clinical Laboratory, Kochi Medical School, Nankoku 783-8505, Japan. E-mail yamasakf@med.kochi-u.ac.jp

Circulation **is available at http://www.circulationaha.org** **DOI: 10.1161/CIRCULATIONAHA.105.587915**

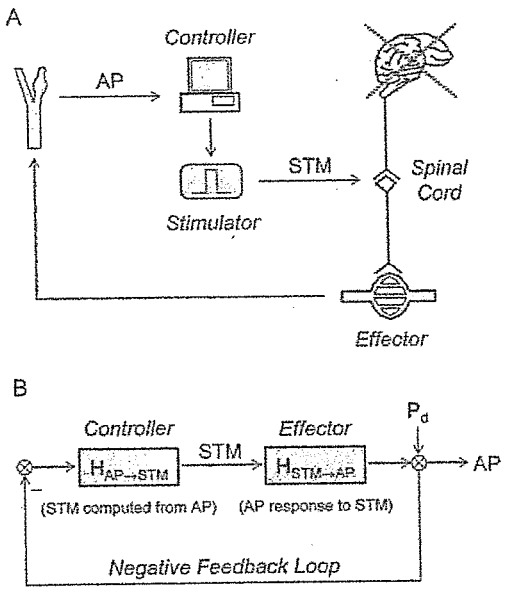

Figure 1. Schematic illustration (A) and block diagram (B) of a BBS. In the context of central baroreflex failure, the BBS automatically computes the frequency (STM) of a pulse train to stimulate sympathetic nerves through an epidural catheter placed at the level of lower thoracic spinal cord, while simultaneously sensing the change in AP. $H_{AP\rightarrow STM}$ denotes a transfer function for the controller functioning as an artificial vasomotor center. $H_{STM\rightarrow AP}$ is a transfer function showing the dynamic response of AP to STM. The overall transfer function of the BBS is given by $H_{AP\rightarrow STM}\times H_{STM\rightarrow AP}$. Therefore, the effect of an external disturbance (P_d) on AP is attenuated to $1/(1+H_{AP\rightarrow STM}\times H_{STM\rightarrow AP})$.

cutes real-time operations that determine the frequency of electrical stimulation (STM) required to minimize the effect of an external disturbance (P_d) on AP and then commands an electrical stimulator to deliver a stimulus of the same frequency to the vasomotor sympathetic nerves via epidural-catheter electrodes placed at the lower thoracic level of the spinal cord. The lower thoracic level was selected as the site for the neural interface of the BBS because the abdominal splanchnic vascular bed is a major effector mechanism for the arterial baroreflex.[23–25]

According to a classic feedback-control theory, ie, feedback correction with proportional and integral gain factors,[26,27] the following algorithm was used to program the controller for the calculation of STM in the frequency domain:

$$H_{AP\rightarrow STM}=K_p+\frac{K_i}{2\pi fj} \quad (1)$$

where $H_{AP\rightarrow STM}$ is a transfer function from AP to STM, K_p is the proportional correction factor, K_i is the integral correction factor, and j is the imaginary unit. The proportional factor determines the feedback amplification based on the absolute value of the instantaneous control error due to P_d, and the integral factor adjusts the feedback amplification based on the cumulative value of the instantaneous control error. Therefore, STM is computed as follows:

$$STM=-AP\cdot H_{AP\rightarrow STM} \quad (2)$$

and AP is also expressed as follows:

$$AP=STM\cdot H_{STM\rightarrow AP}+P_d \quad (3)$$

where $H_{STM\rightarrow AP}$ denotes the frequency response of AP to STM. From Equations 2 and 3, the effect of P_d on AP is estimated as follows:

$$AP=\frac{1}{1+H_{AP\rightarrow STM}\cdot H_{STM\rightarrow AP}}P_d \quad (4)$$

Thus, if $H_{AP\rightarrow STM}\cdot H_{STM\rightarrow AP}$ is far larger than unity, the BBS can nullify the effect of P_d on AP.

Subjects and Experimental Protocols

A total of 33 patients (46 to 84 years old, 19 males) who underwent orthopedic operations were enrolled in the present study. Ten patients had hypertension, and 4 had diabetes mellitus. None of the subjects had frequent ectopic beats or atrial fibrillation. After induction anesthesia with propofol, an endotracheal tube was introduced orally. The patients were mechanically ventilated with 67% nitrous oxide and 1.5% to 2% end-tidal sevoflurane in oxygen during experimental protocols, while end-tidal carbon dioxide was maintained at 35 to 38 mm Hg. An arterial catheter was placed in the radial artery for AP measurement. To record central venous pressure (CVP), a central venous catheter was placed in the femoral vein, and the tip of the catheter was advanced into the inferior vena cava just above the diaphragmatic level. Furthermore, an epidural catheter was placed percutaneously, and the tip, which contained a pair of electrodes (Unique Medical, Tokyo; interelectrode distance 15 mm), was placed at the level of Th_{9-11}. Placement of the central venous catheter and the epidural catheter was verified by chest radiograph.[28]

Before making an incision of affected areas, we performed 2 different protocols in separate groups of patients. In the first group of patients (n=12, 46 to 76 years old, 7 males) undergoing operations for cervical spondylosis and canal stenosis, the averaged $H_{STM\rightarrow AP}$ was estimated and the $H_{AP\rightarrow STM}$ was designed parametrically with Equation 1 to minimize the effect of P_d on AP. After we programmed the designed $H_{AP\rightarrow STM}$ into the computer, the efficacy of the BBS was tested against the rapid progressive hypotension induced by use of a thigh tourniquet[29–31] in the second group of patients (n=21, 64 to 84 years old, 12 males) undergoing operation for knee joint osteoarthritis. During each protocol, the muscle twitches induced by spinal cord stimulation were prevented by the intravenous administration of vecuronium bromide. Analgesia for the pain provoked by spinal cord stimulation and tourniquet inflation was provided by intravenous injection of fentanyl citrate. In a preliminary study, the validity of the analgesic preparation was confirmed for the experimental protocols, and the safety of spinal cord stimulation for 20 minutes was verified.

Estimation of Transfer Function From STM to AP

To characterize the dynamic nature of the AP response to STM, ie, $H_{STM\rightarrow AP}$, the lower thoracic sympathetic nerves were randomly stimulated for 15 minutes while we recorded AP. According to a white noise method for system identification, the STM was altered between 0 and 20 Hz every 4 seconds. The pulse width of electrical stimuli was fixed at 0.1 ms. The stimulation current was adjusted for each patient so as to produce a pressor response of ≈10 mm Hg at 20 Hz. This resulted in an average current of 15±4 (mean±SD) mA. The electrical signals of STM and AP were digitized at 100 Hz. As described previously,[20–22] the transfer function from STM to AP, $H_{STM\rightarrow AP}$, was estimated with a fast Fourier transform algorithm. Finally, the average of $H_{STM\rightarrow AP}$ among 12 patients was calculated.

Design of Artificial Vasomotor Center

With substitution of the averaged $H_{STM\rightarrow AP}$ for Equation 4, the instantaneous AP response to P_d was simulated numerically, and a stepwise decline with an amplitude of 20 mm Hg was imposed on the BBS. While the feedback parameters of $H_{AP\rightarrow STM}$, ie, K_p and K_i, were altered, the effect of the parameters on the AP response was investigated. Finally, the parameters that enabled the BBS to quickly and stably minimize the effect of P_d on AP were determined.

Efficacy of BBS in a Clinical Model of Transient Hypotension

The performance of the BBS was evaluated in a clinical model of rapid transient hypotension (n=21). Rapid hypotension was evoked by the sudden deflation of a thigh tourniquet, which is widely used to achieve bloodless dissection during total knee arthroplasty.[29–31] Acute hypotension immediately after tourniquet release is a well-